Chemical genetics identifies Rab geranylgeranyl transferase as an apoptotic target of farnesyl transferase inhibitors

Mark R. Lackner,[1,3] Rachel M. Kindt,[1,3] Pamela M. Carroll,[2,3] Katherine Brown,[1] Michael R. Cancilla,[1] Changyou Chen,[1] Heshani de Silva,[2] Yvonne Franke,[1] Bo Guan,[2] Tim Heuer,[1] Tak Hung,[1] Kevin Keegan,[1] Jae Moon Lee,[1] Veeraswamy Manne,[2] Carol O'Brien,[1] Dianne Parry,[1] Juan J. Perez-Villar,[2] Rajashekar K. Reddy,[2] Hong Xiao,[2] Hangjun Zhan,[1] Mark Cockett,[2] Greg Plowman,[1] Kevin Fitzgerald,[2] Michael Costa,[1] and Petra Ross-Macdonald[2,*]

[1]Exelixis Inc., 170 Harbor Way, South San Francisco, California 94083
[2]Bristol-Myers Squibb Pharmaceutical Research Institute, PO Box 5400, Princeton, New Jersey 08543
[3]These authors contributed equally to this work.
*Correspondence: rossmacp@bms.com

Summary

A chemical genetics approach identified a cellular target of several proapoptotic farnesyl transferase inhibitors (FTIs). Treatment with these FTIs caused p53-independent apoptosis in *Caenorhabditis elegans*, which was mimicked by knockdown of endosomal trafficking proteins, including Rab5, Rab7, the HOPS complex, and notably the enzyme Rab geranylgeranyl transferase (RabGGT). These FTIs were found to inhibit mammalian RabGGT with potencies that correlated with their proapoptotic activity. Knockdown of RabGGT induced apoptosis in mammalian cancer cell lines, and both RabGGT subunits were overexpressed in several tumor tissues. These findings validate RabGGT, and by extension endosomal function, as a therapeutically relevant target for modulation of apoptosis, and enhance our understanding of the mechanism of action of FTIs.

Introduction

Modern target-based drug discovery begins with the development of highly potent in vitro agonists or antagonists of a disease-associated target. However, agents that appear to have exquisite specificity for their target often yield unexpected biological activities. For example, compounds inhibiting farnesyl transferase (FT) have been developed as anticancer agents on the premise that they should block transforming Ras activity by inhibiting Ras prenylation and membrane association. While the FTIs have shown promise in the clinic, the heterogeneity of responses seen in vivo and lack of correlation to Ras function suggests several mechanisms of therapeutic action (reviewed by Head and Johnston, 2003). The role of other proteins that require farnesylation has come under increasing scrutiny (Prendergast and Rane, 2001). However, the potential role of other direct molecular targets of the compounds has not received widespread attention.

Eukaryotic cells possess two other prenyl transferases, geranylgeranyl transferase I (GGTI) and Rab geranylgeranyl transferase (RabGGT or GGTII). FT and GGTI are the most closely related, sharing a common α subunit and 30% identity in their β subunits. FT and GGTI (known as the CaaX prenylases) both recognize the tetrapeptide motif CaaX at the C terminus of their substrates and modify a single cysteine residue. Their substrates are then further processed by the CaaX endoprotease and the isoprenylcysteine carboxyl methyltransferase (ICMT) (Clarke, 1992). Since GGTI modifies essential cellular proteins such as the Rho family of GTPases (Bishop and Hall, 2000), the development of FTIs has focused on selectivity for FT over GGTI (for example, see Bell et al., 2002; Hunt et al., 2000).

In contrast, the third eukaryotic protein prenylase RabGGT appeared so distinct from the CaaX prenylases that its potential for interaction with the therapeutic FTIs was considered to be low. Like FT and GGTI, RabGGT functions as a heterodimer. The α subunit has 27% identity to that of the CaaX prenylases but contains additional domains, while the β subunit shows 29% identity to that of FT. The protein substrates of RabGGT have heterogeneous C termini that usually contain two cysteine residues (CXC), both of which are modified by geranylgeranyl groups without any subsequent processing steps. Unlike the CaaX prenylases, RabGGT requires specific accessory pro-

SIGNIFICANCE

FTIs were designed to treat tumors by inhibiting the function of the farnesyl transferase (FT) substrate Ras; however, they have activity on cancer cells and tumors that do not contain activated Ras, suggesting additional mechanisms. Using a chemical genetics approach, we have identified the enzyme RabGGT as an additional direct target of several proapoptotic FTIs, and demonstrated that loss of RabGGT function triggers p53-independent apoptosis. These findings will impact the interpretation of in vivo efficacy and toxicity studies of clinical FTIs, and may facilitate patient selection. Our results also point to the development of a new generation of anticancer agents specifically targeting RabGGT.

Table 1. Activity of compounds in enzyme inhibition assays and in cellular assays for apoptosis and reversion

Compound	FT IC_{50} (nM)	Rat1-CVLS (H-Ras): % reversion at 100 nM	HCT116 apoptosis (EC_{50}, μM)	*C. elegans* apoptosis	RabGGT IC_{50} (nM)	RabGGT IC_{90} (nM)
BMS1	7.8	30	++ (0.4)	++	21	200
BMS2	2.4	75	+ (3.3)	+	36	295
BMS3	1.4	90	++ (0.04)	+	16	93
BMS4	1.5	85	+/– (30)	–	540	10 μM

teins known as REPs to guide the interaction with its targets (reviewed by Seabra, 2000). Despite these differences, the three prenylases have strikingly similar active sites (Strickland et al., 1998; Zhang et al., 2000) and mechanisms of substrate modification (Long et al., 2002). The RabGGT substrates identified to date are all members of a family of >60 Ras-related proteins called Rabs. These monomeric GTPases regulate intracellular membrane traffic, and their prenylation is usually essential for correct targeting and function (reviewed by Deneka et al., 2003). New work linking levels of Rab25 to the aggressiveness of epithelial cancers is the first direct evidence that they play an important role in carcinogenesis (Cheng et al., 2004).

During the development of small molecule FTIs at Bristol-Myers Squibb, several compounds were observed to possess a proapoptotic activity that did not correlate with their potency against either FT or GGTI (Rose et al., 2001). Using the nematode *Caenorhabditis elegans,* we undertook a chemical genetics approach to clarify their mechanism of action. These FTIs were found to be proapoptotic in *C. elegans*, which is a well-validated system for studying apoptosis (reviewed by Gartner et al., 2000; Stergiou and Hengartner, 2004). Similar proapoptotic effects were produced in *C. elegans* by targeted knockdown of components of the RabGGT complex and specific members of the Rab family. Additional biochemical and genetic tests established that the proapoptotic activity of these compounds in nematodes and in human cancer cells is related to their inhibition of RabGGT, and implicated this enzyme for the first time in cancer and apoptosis.

Results

Proapoptotic activity of FT inhibitors in *C. elegans*

As germ cells in *C. elegans* progress through meiosis and differentiation to become mature oocytes, some cells undergo programmed cell death (apoptosis) as part of normal development (Gumienny et al., 1999). Although up to 300 oocytes may undergo apoptosis over the life of the animal, the cell corpses are rarely seen in wild-type worms. Since germ cells are competent to undergo apoptosis and can be visualized in an intact animal, the number of corpses provides a sensitive and accurate indicator for apoptotic modulators.

Four BMS compounds with similar levels of FT inhibition but differing potencies in a mammalian apoptosis assay (Table 1; assays as described by Rose et al. [2001]) were selected for evaluation for the phenotype of apoptosis in *C. elegans* germline cells. Worms treated with compound BMS1 showed a striking increase in the number of cell corpses (Figures 1A and 1B). While untreated wild-type adult worms contained at most two apoptotic corpses/gonad, with an average of less than one, worms treated with BMS1 at 0.8 mM had at least two corpses and an average of over six (Table 2A). The effect of BMS1 was similar in degree and appearance to that of RNA interference (RNAi) directed against *ced-9*, a *C. elegans* homolog of the antiapoptotic protein Bcl-2 (Table 2A). The relatively high dose of compound required is consistent with other studies (R.M.K., unpublished; Lewis et al., 1980), and may be due to the worm's protective cuticle. Induction of apoptosis by BMS1 was dose-dependent (Supplemental Figure S1). Compounds BMS2 and BMS3 were also found to increase the level of germline apoptosis, whereas BMS4 had a very minor effect (Figure 2A; Table 2A). Thus, the observations from a mammalian cellular apoptosis assay were recapitulated in the *C. elegans* assay. This correlation persisted for a further series of 8

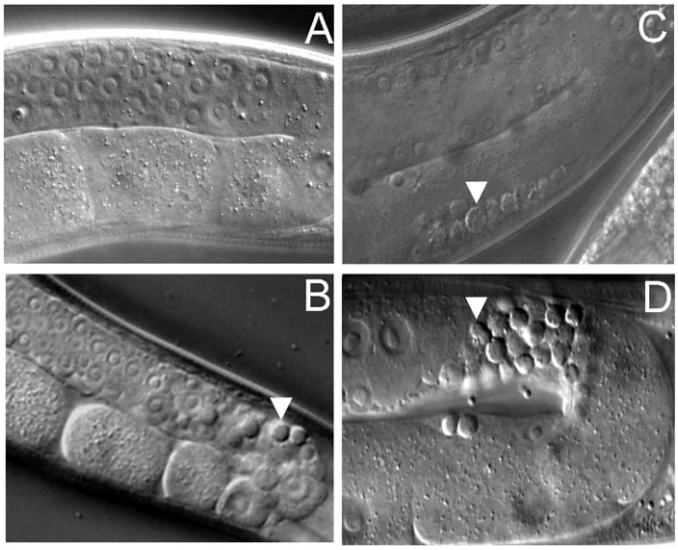

Figure 1. Germline cell apoptosis in *C. elegans*

Nomarski images of the gonad arm region in a one- to two-day-old worm, oriented with the distal region of the gonad to the top. Germ cells proceed in a clockwise direction as they mature. White arrowheads indicate examples of an apoptotic corpse.

A: Wild-type worm, treated with DMSO. No corpses are visible.

B: Wild-type worm, exposed to BMS1 (1.6 mM) for 16 hr. Several corpses are present in the distal region.

C: *ced-1(e1735); ced-10 (n1993)* engulfment mutant worm. A group of degenerating corpses is present in the proximal gonad region.

D: *vps-41(ep402)* mutant worm. A large cluster of corpses is present in the distal region.

Table 2. Effect of compound and/or RNAi treatment on the level of apoptotic corpses in *C. elegans*

	Host strain	Protein name/ORF targeted by RNAi treatment	Compound (dose)	Mean corpses (SD)
A	WT		Vehicle	1.1 (0.8)
	WT		BMS1 (0.8 mM)	6.9 (2.8)
	WT		BMS2 (1.6 mM)	2.0 (1.4)
	WT		BMS3 (1.6 mM)	2.3 (1.6)
	WT		BMS4 (1.6 mM)	1.2 (1.2)
	WT	CED-9/T07C4.8		4.8 (2.4)
B	WT		Vehicle	0.4 (0.8)
	WT		BMS1 (1.6 mM)	6.3 (1.3)
	cep-1		BMS1 (1.6 mM)	5.3 (1.8)
	ced-3		Vehicle	0.1 (0.4)
	ced-3		BMS1 (1.6 mM)	0.1 (0.3)
	ced-4		Vehicle	0.0 (0.0)
	ced-4		BMS1 (1.6 mM)	0.2 (0.4)
C	*cep-1*	mock		0.6 (0.8)
	cep-1	VPS-11/R06F6.2		22.0 (8.5)
	cep-1	VPS-16/C05D11.2		15.1 (6.3)
	cep-1	VPS-18/W06B4.3		15.3 (4.4)
	cep-1	VPS-33/Y75B8A.24		5.3 (2.0)
	cep-1	VPS-39/T08G5.5		10.1 (5.1)
	cep-1	RAB-5/F26H9.6		10.9 (4.0)
	cep-1	RAB-7/W03C9.3		18.2 (6.4)
	cep-1	RAB-18/Y92C3B.3		1.0 (0.7)
D	*cep-1*	RabGGT-α/M57.2		5.5 (2.7)
	cep-1	RabGGT-β/B0280.1		16.9 (6.4)
	cep-1	Rab GDI/Y57G11C.10		13.6 (6.0)
	cep-1	FT-α/GGT1-α/R02D3.5		2.6 (1.6)
	cep-1	FT-β/R23B12.6		1.6 (0.8)
	cep-1	GGT1-β/Y48E1B.3		0.9 (1.1)
	cep-1	CaaX protease/C04F12.1		1.2 (0.9)
	cep-1	ICMT/F21F3.3		0.7 (0.8)
E	WT		Vehicle	0.7 (0.7)
	WT		BMS1 (0.3 mM)	2.3 (1.8)
	WT	RabGGT-α/M57.2	Vehicle	2.7 (1.5)
	WT	RabGGT-α/M57.2	BMS1 (0.3 mM)	8 (3.0)
	WT	Control ORF	Vehicle	2.8 (2.0)
	WT	Control ORF	BMS1 (0.3 mM)	2.1 (1.3)

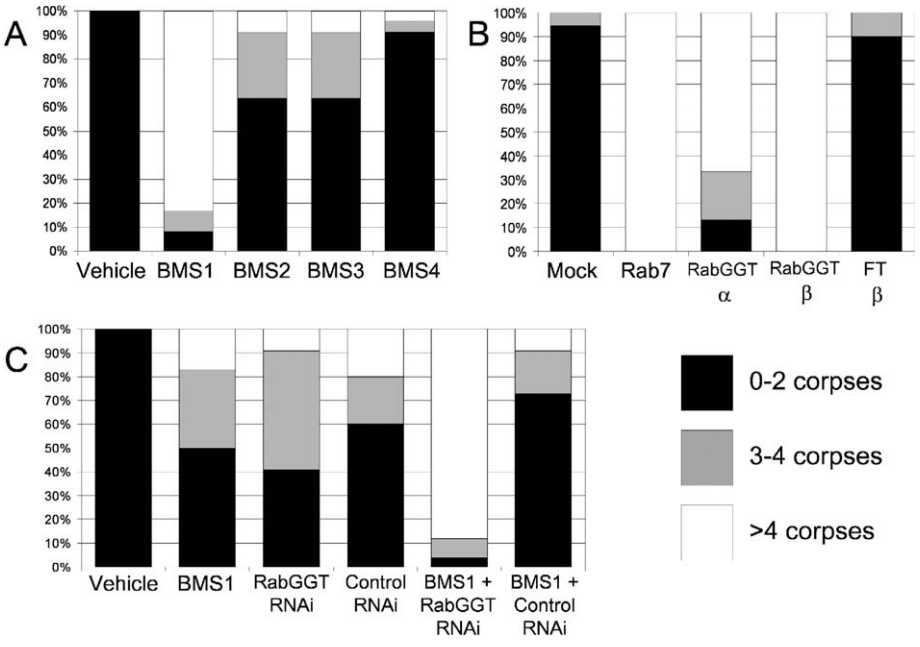

Figure 2. Effect of compound treatment and RNAi on levels of apoptosis in *C. elegans* germline cells

Each column shows percentage of worms in the sample population that contained two or fewer corpses (black), three or four corpses (gray), or more than four corpses (white). Values were derived from representative experiments using 10–24 animals per treatment.

A: Wild-type worms treated for 16 hr with compounds BMS1 through BMS4 at 0.8 mM.

B: *cep-1(ep347)* mutant worms were treated with RNAi directed against mRNA for RAB-7 or the RabGGT subunits or FT-β, as indicated.

C: Wild-type worms were treated with compound BMS1 at 0.3 mM, or RNAi against RabGGT-α, or both. The effects of the combined treatment are more than the additive effects of each individual treatment. The effect of RNAi against an unrelated target, both alone and in combination with BMS1, is also shown.

FTI compounds (data not shown), indicating that the cause of apoptosis was mechanistically related in the two species.

Proapoptotic effects are p53-independent but require a functional caspase pathway

In addition to developmentally programmed apoptosis, germ cells in *C. elegans* can undergo DNA damage-induced apoptosis through a conserved checkpoint pathway that requires p53 function (Derry et al., 2001; Gartner et al., 2000; Schumacher et al., 2001). No reduction of the proapoptotic effect of BMS1 was observed upon treatment of a p53 deletion (*cep-1*) mutant strain of *C. elegans* (Table 2B), indicating that the compound action was p53-independent.

To investigate whether the apoptotic effects of the BMS compounds in *C. elegans* were mediated via the canonical caspase pathway, compound BMS1 was applied to worms carrying mutations in either *ced-3* (caspase) or *ced-4* (APAF1). While treatment of wild-type worms with BMS1 increased the number of corpses to an average of over six per arm, no increase in corpses was observed when the *ced-3* or *ced-4* mutants were treated (Table 2B). This suggests that the corpses observed in BMS1-treated worms were derived via the established apoptotic mechanism.

An observed increase in apoptotic corpses could be due to either a defect in the apoptosis process itself or to a failure to engulf and clear the apoptotic corpses from the gonad (reviewed by Hengartner, 2001). We examined the gonad arm region in a worm strain carrying both the *ced-1* and *ced-10* mutations, leading to absence of engulfment. The corpses in this strain showed a characteristic vacuolated morphology that was distinct from that of corpses produced by RNAi against *ced-9* (Bcl-2), and they accumulated in the proximal region of the gonad arm (Figure 1C), where they persisted indefinitely. Since the corpses in BMS compound-treated worms were not concentrated in the distal region and did not appear vacuolated (Figure 1B), and disappeared over time (data not shown), the compound-induced increase in the number of corpses was likely due to an increase in apoptosis per se, rather than a failure to engulf the corpses that arise.

Genetic screens implicate Rab Proteins and RabGGT in apoptosis

In parallel with our studies using compounds, EMS mutagenesis and RNA interference (RNAi) screens were conducted to identify key mediators of germline apoptosis in *C. elegans*. Since we were interested in regulators that act in the absence of a functional p53 protein (which is mutated in many cancers; Slee et al., 2004), we looked for genes whose inactivation resulted in an increase in the number of apoptotic cells in a *cep-1* deletion mutant.

In a forward genetic approach, approximately 58,000 F2 and 100,000 F1 EMS-mutagenized genomes were screened, and four loci were identified. For the mutant that showed the strongest increase in germline apoptosis, *ep402*, adults typically displayed >20 apoptotic corpses per gonad arm (Figure 1D). *ep402* also caused phenotypes not associated with apoptosis, including maternal-effect embryonic lethality and partially penetrant larval arrest. The increased apoptosis in the *ep402* mutant was p53-independent, but was blocked by a *ced-4*/APAF1 loss-of-function mutation (data not shown). Molecular genetic analysis revealed that the predicted genes *Y34B4A.1* and *F32A6.3* were in fact a single locus, which we named *vps-41*, that was affected by the *ep402* mutation. *vps-41* encodes a 901 amino acid protein that is orthologous to yeast Vps41 (29% identical and 54% similar over 179 amino acids) and human VPS41 (28% identical and 50% similar over 842 amino acids). In *Saccharomyces cerevisiae*, Vps41 is required for sorting of proteins to the vacuole/lysosome, specifically for the step of endosomes and autophagosomes docking to lysosomes prior to vesicle fusion (Nakamura et al., 1997). *C. elegans* VPS-41 contains both the clathrin heavy chain repeat and the RING-H2 zinc finger domains present in human VPS41. The *ep402* allele was found to be a nonsense mutation that truncated both these domains.

In addition to the forward-genetic approach, RNAi treatment was used to screen for genes for which a reduction of function caused an increase in germline apoptosis in a *cep-1* deletion background. We used a focused set of RNAi reagents comprising 2,636 genes that included the majority of kinases, phosphatases, proteases, and nonolfactory G protein-coupled receptors encoded in the *C. elegans* genome. Since we had identified the *C. elegans* homolog of *VPS41* in the previous screen, indicating that endosome-lysosome protein sorting or autophagy (degradation of cytoplasmic proteins and organelles) may play a role in apoptosis, we also screened RNAi reagents for a set of 70 *C. elegans* genes that were related to genes implicated in lysosomal trafficking and/or autophagy in yeast. From this panel of 2706 genes, we identified 18 genes for which RNAi knockdown resulted in elevated levels of germline apoptosis. Several of these genes will be described elsewhere. Although the effect of the RNAi treatment varied in penetrance and expressivity from gene to gene, in each case, the proapoptotic effects were seen in both wild-type and p53 mutant backgrounds, and were *ced-3*/caspase- and *ced-4*/APAF1-dependent (data not shown). Because apoptotic regulators of interest were to be validated in a mammalian cell-autonomous system (as shown in Figure 4), they were not rigorously tested for effects on the *C. elegans*-specific engulfment and disposal pathways. However, in each case, it was observed that the phenotype did not resemble existing engulfment mutants (compare Figures 1C and 1D).

Among the genes that most strongly induced apoptosis in this RNAi knockdown screen, we noted orthologs encoding the five proteins (Vps11, Vps16, Vps18, Vps33, Vps39; Table 2C) that combine with Vps41 to form the HOPS complex in yeast. The HOPS complex interacts with the GTPase Rab7, and together they are required to drive endosome-lysosome and autophagosome-lysosome docking and fusion (Seals et al., 2000). Inactivation of the *C. elegans* ortholog of *RAB7*, *rab-7*, also led to high levels of germline apoptosis (Table 2C). However, RNAi of homologs of yeast autophagy-specific genes did not induce germline apoptosis, suggesting that endosome-lysosome function was of primary relevance. We examined the effect of inactivating the 28 other Rab family members identified in the *C. elegans* genome. Only RNAi of *rab-7* and *rab-5* (the single *C. elegans* ortholog of the human *RAB5A*, *RAB5B*, and *RAB5C* genes) was found to induce germline apoptosis (Table 2C). Rab5 and Rab7 share a function in protein trafficking from early endosomes to late endosomes. RNAi against the single *C. elegans* ortholog of the mammalian Rab guanine nucleotide dissociation inhibitors GDI1 and GDI2, which are positive regulators of Rab function, also induced high levels of

germline apoptosis (Table 2D). Next, we examined inactivation of the enzyme responsible for prenylation of the Rab GTPases. RNAi directed against mRNA for either the *C. elegans* RabGGT-α or RabGGT-β subunit was effective at inducing germline apoptosis. In contrast, RNAi treatment directed against *C. elegans* genes encoding either the FT-β or GGTI-β subunit, the α subunit shared by FT and GGTI, or other components of the CaaX processing system, did not result in increased apoptosis in this assay (Table 2D). The finding that a reduction of *RabGGT* expression caused increased apoptosis, in conjunction with the known functional and structural similarities between this enzyme and FT, led us to consider that RabGGT could be a target of the proapoptotic FTI compounds BMS1, BMS2, and BMS3.

Synergistic effect of compound treatment with loss of RabGGT

We examined the effect of a low dose of BMS1 (0.3 mM) on the level of apoptosis caused by a reduction in *RabGGT* expression. The experimental rationale is that the effect of a submaximal compound dose will be potentiated if the target's activity is already partially compromised. RNAi directed against the α subunit of RabGGT (*RabGGT-α* RNAi) induced a lower level of germline apoptosis than RNAi directed against the β subunit (Figure 2B, Table 2E), suggesting that it reduced but did not eliminate RabGGT activity. Therefore, *RabGGT-α* RNAi was used to produce a partial loss of RabGGT function in adult worms. Table 2E contains data for each treatment administered individually and in combination with compound. Coadministration of the *RabGGT-α* RNAi reagent with BMS1 at 0.3 mM caused an increase in the level of apoptosis that was substantially greater than the additive value of the independent treatments: the fraction of gonad arms with more than 4 corpses increased to 88%, from 9% with the RNAi treatment alone or 17% with the low dose of compound alone. No such synergy was seen between compound treatment and a control RNAi treatment of an unrelated target that produced a similar level of apoptosis (Table 2E, Figure 2C). Thus, a specific hypersensitivity to the compound was observed when *RabGGT* expression was reduced.

Direct inhibition of RabGGT activity by the FTI compounds

The synergism of the FTI compounds with RNAi against *RabGGT* was suggestive of compound inhibition of RabGGT activity. We examined this possibility by using an in vitro assay that reconstituted the prenylation of Rab3A by RabGGT. The proapoptotic compounds BMS1, BMS2, and BMS3 were found to be highly potent inhibitors of mammalian RabGGT, with IC_{50} values of 16–36 nM. Compound BMS4 was up to 33-fold less potent, with an IC_{50} of 541 nM. Thus, there was an agreement between the relative activity of these compounds in apoptosis assays and their inhibition of RabGGT activity in vitro (Table 1). Dose response curves differed, which is relevant if it is necessary to completely eliminate the function of RabGGT to produce apoptosis. For example, compound BMS1 had an IC_{90} value of 200 nM, whereas BMS4 was 50-fold less potent, with an IC_{90} of 10 μM (Figure 3A and Table 1). BMS1 has been tested at 8 μM or higher on 69 other pharmaceutical targets with no inhibition of activity, indicating that its action on RabGGT is specific.

To further investigate the occurrence of dual inhibition and its relationship to the proapoptotic activity, an additional 19 potent FTI compounds (FT IC_{50} for H-ras <20 nM) were evaluated in both assays. The majority of these FTIs were found to also inhibit RabGGT: 14 compounds had IC_{50} values below 100 nM, and the IC_{50}s ranged from 8 nM to >15 μM. These observations further supported a relationship between the potency of a compound for inhibition of RabGGT (IC_{90}) and its ability to induce apoptosis (Figure 3B; $R^2 = 0.76$). To extend these observations, 12 FTIs with a RabGGT IC_{90} range of 58 to 570 nM were tested for apoptotic activity across eight further cell lines, including the p53-negative PC3 and MLF lines. In general, the compounds induced apoptosis at submicromolar concentrations, with the least potent RabGGT inhibitor also being the least potent apoptotic agent (Supplemental Table S1; $R^2 > 0.54$ for seven lines). In contrast, no relationship between potency against FT and apoptotic activity was observed for these compounds (Supplemental Table S1; $R^2 < 0.23$).

To investigate whether cellular activity against RabGGT occurs at doses relevant to the proapoptotic effects of compounds, the A549 human lung cancer cell line was treated with compounds BMS1 and BMS4. Cellular inhibition of RabGGT and FT was detected by the cytoplasmic accumulation of unprenylated Rab5B or unprenylated H-Ras, respectively. Both BMS compounds maximally inhibited H-Ras prenylation at the lowest dose used (Figure 3C). In the same extracts, accumulation of unprenylated Rab5B in BMS1-treated cells was evident at the 0.5 μM dose and increased at the 1μM dose, while for BMS4 no accumulation relative to control treatment was apparent at doses up to 5 μM (Figure 3C). To determine whether apoptosis was induced by these treatments, activation of caspase-3/7 was monitored by the appearance of a luminescent cleavage product. Staurosporine treatment was included as a positive control. Caspase activation was induced by BMS1 at both 0.5 μM and 1 μM, but was not seen with BMS 4 at doses up to 5 μM (Figure 3D). The observation of a >10-fold difference between the cellular potency of BMS1 and BMS4 for both RabGGT inhibition and induction of caspase activity supports a relationship between these properties. These assays also reiterate the lack of relationship between potency against FT and apoptotic activity for these compounds.

Targeting RabGGT by siRNA induces apoptosis in mammalian cancer cell lines

If inactivation of RabGGT by compounds BMS1, BMS2, and BMS3 is a source of their proapoptotic activity in mammalian cancer cells, then a reduction of RabGGT function by other means should also induce apoptosis. We induced degradation of *RabGGT* mRNA using small interfering RNAs (siRNA), and examined the effects on apoptotic status of cancer cell lines. For each RabGGT subunit, two effective siRNAs were selected (Supplemental Figures S2 and S3). An siRNA targeting the caspase regulator XIAP was also used, providing a benchmark for induction of apoptosis. siRNAs against both α and β subunits were antiproliferative (Supplemental Figure S4). Apoptotic status was evaluated both by measurement of apoptotic indi-

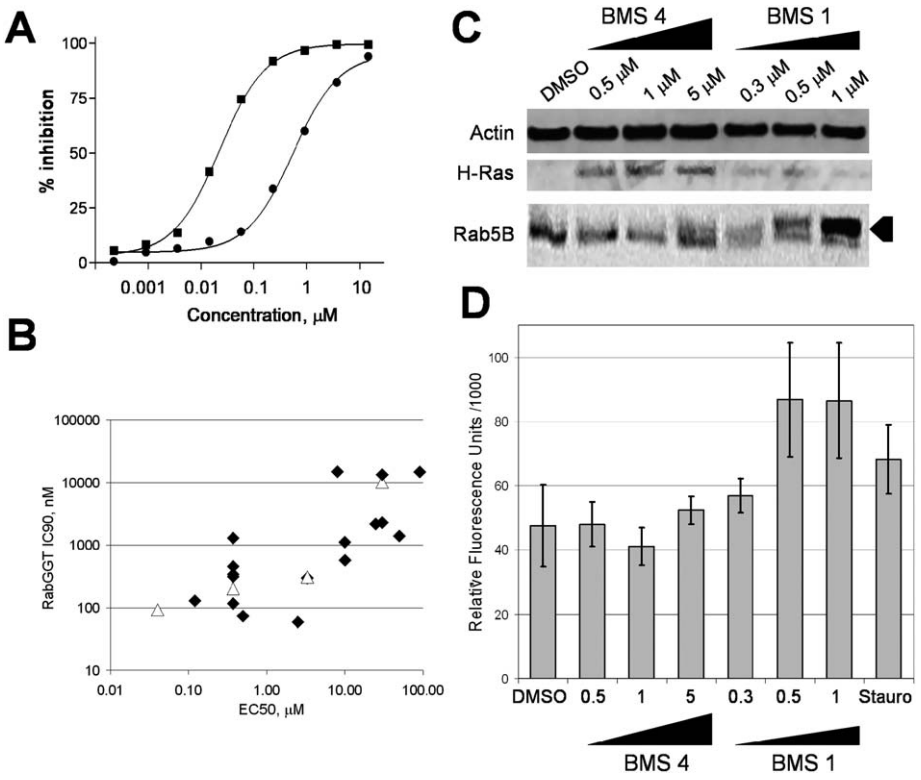

Figure 3. Inhibition of RabGGT prenylation activity by multiple FTIs, and relationship to their apoptotic activity

A: Representative dose response of RabGGT inhibition by BMS compounds. ■, BMS1 (potent inhibition); ●, BMS4 (weaker inhibition).

B: Levels of apoptotic activity and RabGGT inhibitory activity of a series of FTI compounds. The minimum concentration that produced 50% apoptosis (EC50) was determined on the HCT-116 line. Four compounds with an IC_{90} that exceeded the assay limit (15 μM) are represented at 15 μM. Compounds BMS1–BMS4 are indicated by △.

C: Western blots of cytoplasmic extracts from A549 cells treated for 20 hr as indicated. The cytoplasmic accumulation of H-Ras (center panel) and the appearance of Rab5B with decreased mobility (lower panel, arrow) are diagnostic for lack of prenylation of newly synthesized protein.

D: Caspase-3/7 activation measured by accumulation of a fluorescent cleavage product in A549 cells after 23 hr of compound treatment as indicated (doses are in μM). Staurosporine at 300 nM provides a positive control. The average and standard deviation of replicate assays are shown.

cators in cancer cell populations and by direct observation of individual cells.

First, activation of caspase-3/7 was monitored by the appearance of a luminescent cleavage product after siRNAs were introduced into A549 cells. *RabGGT*-specific siRNAs produced significant increases in signal over the background values for cells transfected with a control siRNA (Figure 4A). The induction of caspase 3/7 activity by *RabGGT* siRNAs was comparable to that of the *XIAP* control, and could be reversed by cotreatment with the caspase inhibitor Z-VAD-FMK (Figure 4A). Second, the occurrence of cytoplasmic histone-associated DNA fragments (a feature of apoptosis; Salgame et al., 1997), was assayed after the siRNAs were introduced into the A2780 human ovarian carcinoma cell line. The siRNAs to *RabGGT* produced a significant signal in this assay, while cells transfected with a control siRNA had the expected background signal (Figure 4C). Finally, activation of caspase 3, nuclear condensation, and proliferation was quantified at two timepoints in individual cells of the p53 null prostate cancer cell line PC3 (Supplemental Tables S2–S4). Activated caspase 3 was seen in a substantial proportion of cells; the effect of *RabGGT* loss was stronger than that of the positive control *XIAP* (Figure 4C). Increased nuclear condensation was seen with siRNAs against *RabGGT* and the *XIAP* control (Figures 4D–4G), with highly compact nuclei found in caspase-positive cells (Figures 4F and 4G). In summary, the positive results seen for several apoptotic parameters in three different cell lines demonstrate that a reduction in RabGGT function can be sufficient to induce cancer cell lines to undergo p53-independent apoptosis.

RabGGT mRNA is overexpressed in a subset of human tumors

Using quantitative reverse transcription-polymerase chain reaction analysis (qRT-PCR), we measured expression of the *RabGGT-α* and *-β* subunits in 9 different tumor types: breast, colon, head and neck, kidney, lung, melanoma, ovary, prostate, and uterine. Matched normal samples were assayed for 169 of the 194 tumor specimens. We found that both *RabGGT-α* and *RabGGT-β* were expressed abundantly in all tissues examined. *RabGGT-β* showed significant overexpression relative to normal tissue in ovarian tumors, adenocarcinomas of the colon, large cell lung carcinomas, and melanomas (Kruskal-Wallis rank statistical analysis with $p < 0.05$; Figure 5). *RabGGT-α* transcripts were also significantly elevated in ovarian tumors and melanomas ($p < 0.05$; data not shown).

Discussion

In this work, the nematode *C. elegans* was used as a surrogate genetic system to identify the mammalian target responsible for the proapoptotic activity of a number of compounds that had been optimized for inhibition of FT. After establishing that the compounds were also proapoptotic in *C. elegans*, we noted a similarity between this compound-induced phenotype and that produced by RNAi of a class of genes identified in a genetic screen. This class encodes proteins involved in vesicular trafficking, and most notably the prenyltransferase RabGGT, which is responsible for geranylgeranylation of the Rab family of small GTPases. In worms, the proapoptotic effect of the compounds is synergistic with a reduction in RabGGT function. Extending our observations from *C. elegans*, we demonstrated

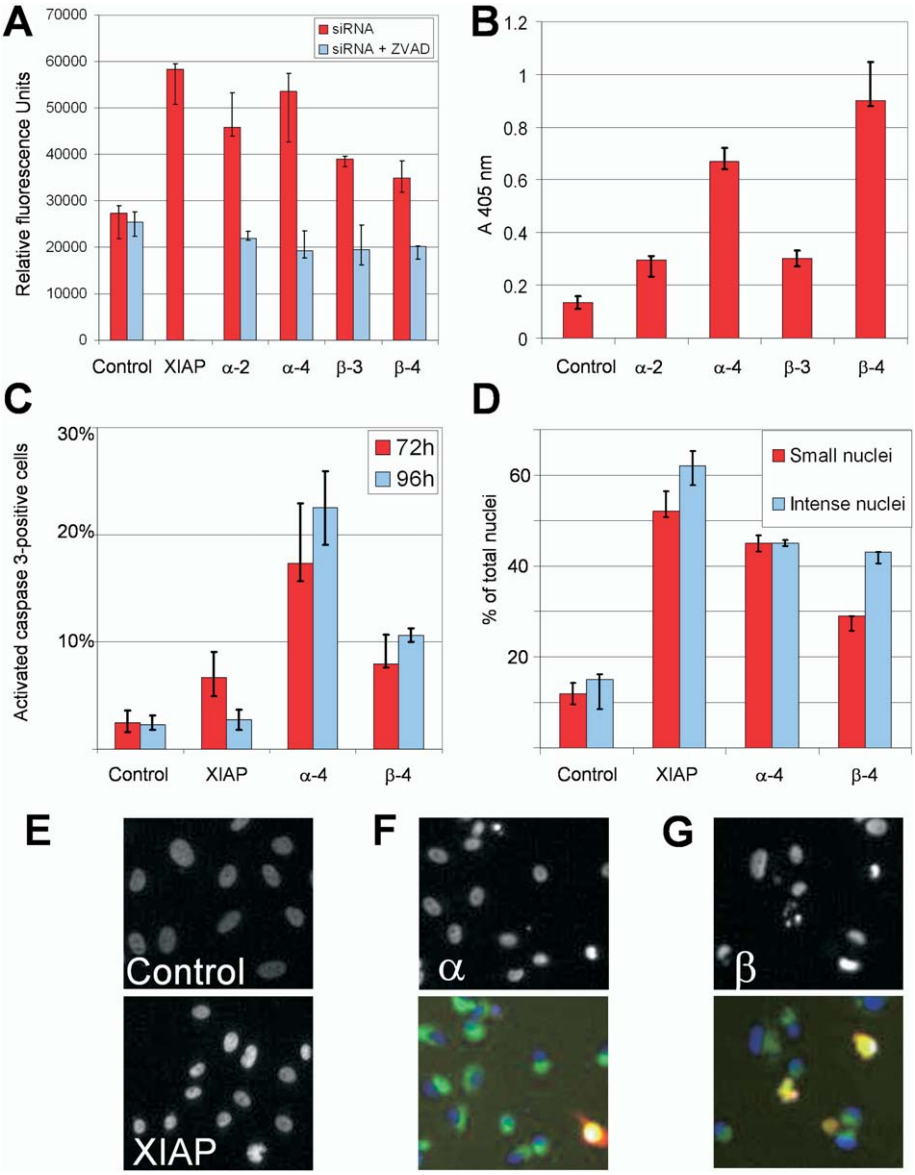

Figure 4. Activation of apoptosis in mammalian cancer cell lines by siRNA directed against RabGGT subunits

The median value and range of replicate assays are shown. Control: siRNA against firefly luciferase. XIAP, siRNA against the caspase regulator *XIAP*. α-2, α-4, siRNAs against *RabGGT-α*. β-3, β-4: siRNAs against *RabGGT-β*.

A: Caspase-3/7 activation measured by accumulation of a fluorescent cleavage product in A549 cells, 28 hr posttransfection. Inhibition of activation by Z-FAD-VMK is also shown.

B: Detection of nucleosomal DNA in cytoplasm of A2780 cells, 48 hr posttransfection.

C: Positive staining for activated caspase 3 in PC3 cells, 72 and 96 hr posttransfection.

D: Quantification of small or bright nuclei in PC3 cells, 96 hr posttransfection.

E: Nuclei of PC3 cells, 96 hr posttransfection with the indicated siRNA.

F and G: Staining of PC3 cells, 96 hr posttransfection with siRNAs against indicated RabGGT subunit. Nuclear DNA is identified with Hoechst (blue). Cells positive for both activated caspase 3 (rhodamine) and cytochrome C (fluorescein) appear yellow.

that the compounds inhibit mammalian RabGGT activity in vitro and in cells with high potency. Cellular inhibition of Rab prenylation was evident at doses that induce apoptosis, and siRNA against *RabGGT* was sufficient to induce apoptosis in three human cancer cell lines. Finally, the *RabGGT-α* and *-β* genes are overexpressed in ovarian tumors and melanomas. In summary, our experimental results illustrate the use of pharmacological, biochemical, and genetic methods that have converged upon a single enzyme. These approaches have identified a novel pathway for p53-independent induction of apoptosis, and suggest that blocking the posttranslational modification of Rab proteins is a source of the proapoptotic activity of some FTIs.

Involvement of the endosomal trafficking pathway in apoptosis

Regulation of endosomal-lysosomal trafficking emerged as a common theme from our genetic screens for proapoptotic mutations in *C. elegans*, suggesting a key role for this organelle in the induction of apoptosis. Endosomal Rab GTPases have very recently been connected to apoptosis and proliferation of cancer cells (Cheng et al., 2004). Our screens identified all known members of the HOPS complex, which acts with Rab7 to regulate endosomal fusion events. We found that knockdown of the *C. elegans* Rab GDI also induced high levels of germline apoptosis, presumably by blocking recycling of GDP-bound Rab proteins from acceptor vesicle membranes back to donor membranes (Pfeffer et al., 1995). The apoptotic function of RabGGT is likely linked to its role in allowing proper membrane localization of the GTPases Rab5 and Rab7, and possibly other Rab family members in mammals. Interestingly, the proapoptotic effect of the FTI compound L-744,832 has been demonstrated to require Amphiphysin II (Bin1; DuHadaway et al., 2003), a protein that functions in endocytosis and is predicted to interact with small GTPases.

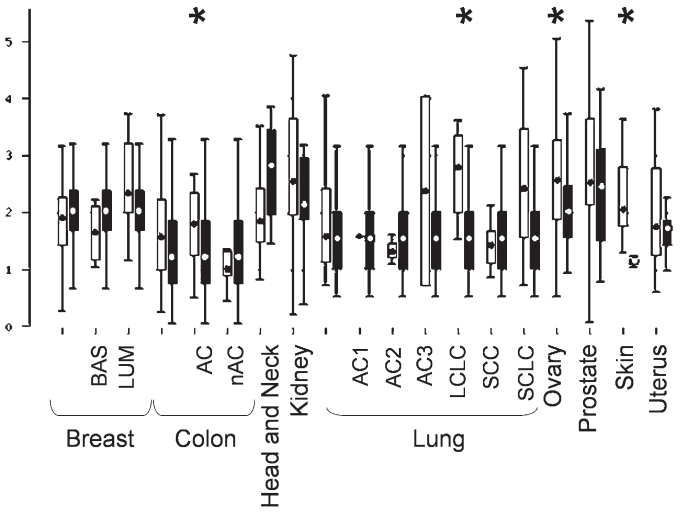

Figure 5. RabGGT-β mRNA is overexpressed in colon, lung, skin, and ovarian tumors

RabGGT-β mRNA levels were using qRT-PCR; asterisks indicate differential expression relative to the corresponding normal tissue ($p < 0.05$ in the Kruskal-Wallis rank statistical analysis). Filled box: normal tissue samples. White box: tumor samples. Circles represent the median, while box boundaries represent the interquartile range. Whiskers extend to the observed values that lie closest to the values calculated by extending the box boundaries by 1.5 times the interquartile range. Expression values are in relative quantity units on a linear scale (see Experimental Procedures). Breast/BAS, basal cell-like; breast/LUM, luminal cell-like; colon/AC, adenocarcinoma; colon/nAC, nonadenocarcinoma; lung/AC1 through AC3, adenocarcinoma subtypes 1 through 3; lung/LCLC, large cell lung carcinoma; lung/SCC, squamous cell carcinoma; lung/SCLC, small cell lung carcinoma.

How does blocking endosomal-lysosomal trafficking induce apoptosis? We envision two general models. First, the lysosome could act directly on established components of the pathway. In support of this model, an antisense knockout of the lysosomal protease cathepsin L lowers Bcl-2 expression levels and triggers apoptosis in human glioma cell lines (Levicar et al., 2003). Similarly, we find that RNAi of the *C. elegans* cathepsin L ortholog, *cpl-1*, induces caspase-dependent germline apoptosis (data not shown). Alternatively, perturbing the fusion of endosomes to lysosomes might indirectly induce apoptosis. In this model, rupture or leakage of accumulated, unfused vesicles might release proapoptotic agents, such as ceramide or hydrolytic enzymes, into the cytoplasm.

Identification of novel targets in cancer

The identification of pro- and antiapoptotic target proteins is an important area of pharmaceutical research (reviewed by Makin, 2002). The work presented in this paper demonstrates that reducing the levels of proteins in the HOPS complex or inhibiting the prenylation of the key regulatory GTPases Rab5 and Rab7 leads to p53-independent induction of programmed cell death. p53 is frequently mutated in human tumors, and studies in a variety of species have indicated that induction of apoptosis (as opposed to cell cycle regulation) is the most conserved function of p53 (reviewed by Slee et al., 2004). By screening for genes whose inactivation triggers apoptosis in the germline of animals lacking *cep-1*/p53, we were able to identify potential drug targets that could have therapeutic benefits in treatment of p53– tumors.

The enzyme RabGGT presents a chemically tractable new target for apoptotic induction in cancer cells. We show that expression of the genes encoding RabGGT subunits is elevated in certain tumor types, indicating that the enzyme may play a functional role in cancer initiation or progression. The RabGGT enzyme structure has been determined, and its mechanism of substrate modification has been studied (Shen and Seabra, 1996; Thoma et al., 2001a; Thoma et al., 2001b; Zhang et al., 2000). A recent study that identified structural factors influencing FTI compound specificity (Reid and Beese, 2004) will provide useful insights for RabGGT inhibitor development. Thus, there is an excellent foundation for a rational drug design approach. Only two compounds that affect RabGGT activity have previously been described, and neither shows a high degree of potency or specificity for RabGGT (Ren et al., 1997; Coxon et al. 2001). Our results demonstrate a strong link between RabGGT function and apoptosis in human cancer cells. Interestingly, no broad proliferation or apoptotic effects were described in mice whose RabGGT-α subunit is impaired (Detter et al., 2000), suggesting that tumor cells could be hypersensitive to the proapoptotic effects of enzyme inhibition. Deficiencies in RabGGT function have, however, been linked to blood clotting abnormalities and retinal degeneration (reviewed by Seabra et al., 2002). The development of specific inhibitors for RabGGT will facilitate the continued characterization of this enzyme's role in apoptosis and other physiological processes.

The role of RabGGT substrates in apoptosis and cancer is also of interest. Recent data on Rab25 implicates endosome recycling in development of epithelial cancers (Cheng et al., 2004). Our genetic screens in worms implicated the endosomal regulators Rab5 and Rab7 in apoptosis. Rab5 regulates transport from the plasma membrane to early endosomes and endosome-endosome fusion, and has been implicated in growth control in a number of studies. The Rab5 effector AAPL1 is essential for cellular proliferation (Miaczynska et al., 2004), while the tumor suppressor gene TSC2 has been reported to act as a GAP for Rab5 (Xiao et al., 1997) and overexpression of the TSC2 GAP domain was found to suppress tumorigenesis (Jin et al., 1996; Momose et al., 2002). In contrast, overexpression of PRC17, also a Rab5 GAP, induces tumorigenesis in nude mice (Pei et al., 2002). Thus, the connection between GTP cycling by Rab5 and tumorigenesis is not yet clear. Rab7 catalyzes late endosome-lysosome and homotypic (endosome-endosome and lysosome-lysosome) fusion. Recently, Edinger et al. (2003) found that an RNAi against *Rab7* slightly improved the survival of a growth factor-deprived murine cell line. This discrepancy with the strongly proapoptotic effect of *rab-7* knockdown seen in *C. elegans* may be due to the different experimental endpoint. It is also possible that despite the good agreement between *C. elegans* and mammalian apoptosis assays that is seen for RabGGT, loss of Rab7 would not induce apoptosis in a mammalian system. Overall, further studies of Rab5 and Rab7 function in cancer models will be required to evaluate their utility as targets for cancer therapy.

Implications for specificity of other FTIs

Our data provide the first demonstration of high-potency dual inhibition of RabGGT and FT. Thoma et al. had raised concerns

over FTI specificity upon noting that RabGGT can effectively bind and transfer farnesyl pyrophosphate (Thoma et al., 2000). However, since the current generation of FTIs occupy the peptide binding site rather than competing for isoprenoid binding (see Reid and Beese, 2004), such crossreactivity had seemed unlikely. Yet the peptide binding site also shows remarkable structural conservation between the three protein prenyltransferases (Zhang et al., 2000). Could the ability to crossreact be a general property of FTIs? Of the 23 FTIs tested in this study, 17 were found to be highly potent inhibitors of RabGGT, indicating that crossreactivity is common but not universal. The 23 compounds have several similarities to clinical candidate FTIs. They are targeted to the peptide binding site by an imidazole ring that acts as a ligand for the zinc ion present in all three enzymes. Imidazole rings have been used for this purpose in several other FTIs in development, for example in Janssen's R115777 (Venet et al., 2003), in Abbott Laboratories' biphenyl FTI (Curtin et al., 2003), in the original Merck clinical compound L-778,123 (Britten et al., 2001), and in Merck's series of macrocyclic compounds (Bell et al., 2002). Additionally, the compounds we tested are predicted to share the common binding attributes identified by Reid and Beese in their study of six diverse clinical FTI candidates (Reid and Beese, 2004). This study also noted that compound selectivity for FT over GGTI does not depend on the peptide substrate specificity of each enzyme. Thus, the difference in RabGGT peptide substrate specificity is not a barrier to crossreactivity by these FTIs. We have found dual inhibition of FT and RabGGT by multiple compounds with diverse structures, indicating that it is not unusual for a compound to interact with both proteins. While our data indicate that the optimization of a compound for inhibition of FT is not directly linked to potency against RabGGT, it is likely that additional FTI compounds fortuitously also inhibit RabGGT. Our data suggest that the role of RabGGT inhibition in the mechanism of action of other proapoptotic FTIs should be evaluated.

Implications for cancer therapy

This work demonstrates that compounds developed as FT inhibitors can also be potent inhibitors of RabGGT. These results have several important implications for the clinical development of FTI drugs, which were conceived as specific therapeutics for Ras-related cancers. First, crossreactivity to a second protein target could explain why FTIs can show activity on tumors and cells that lack transforming Ras function. This discrepancy has provoked research that implicated other FT substrates such as RhoB (Du et al., 1999a) centromere associated proteins (Ashar et al., 2000), and most recently Rheb (Tee et al., 2003). Our data show that such research must also consider activities beyond FT inhibition. Second, our demonstration that inhibition of RabGGT function is proapoptotic may relate to the unexpected proapoptotic effects that have been reported for several FTIs (Du et al., 1999b; End et al., 2001; Jiang et al., 2000; Rose et al., 2001; Manne et al., 2004). Finally, even low potency against RabGGT could be relevant in an FTI treatment setting where high local drug concentrations are achieved. Thus, our findings may explain and help to manage the dose-limiting toxicities that have emerged in clinical trials of these therapeutics (Head and Johnston, 2003). Understanding the mechanism of action of the FTIs will allow improvements in patient selection and in monitoring of in vivo efficacy and toxicity, and may lead to the development of a new generation of agents specifically targeting RabGGT.

Chemical genetics is most commonly framed as an open-ended program to create small molecule modulators of many different proteins as research tools (Strausberg and Schreiber, 2003). Our work highlights the value of combining genetics and biochemistry in focused studies to elucidate the in vivo mechanism of single, well-characterized compounds. This approach may identify novel regulatory mechanisms of important biological processes, and also directly assists the development and clinical use of the resulting drugs. We expect that such studies will become increasingly important as the standards imposed on drug selectivity continue to rise, and as the use of pharmacogenomic tools to match drug and patient becomes more common.

Experimental procedures

Compound treatment and phenotypic analysis of *C. elegans*

The compounds used in this study (Supplemental Figure S5) were dissolved in dimethyl sulfoxide (DMSO) and mixed with dead OP50 bacteria suspended in M9 buffer (Epstein and Shakes, 1995) at a final DMSO concentration of 4%. This suspension was applied to agar plates, which were then seeded with 1-day-old adult worms. Apoptosis was quantified at 16 hr with high-resolution Nomarski optics. Corpses were readily distinguished by their compact, button-like appearance (Gumienny et al., 1999). *ced-3(n2433)* and *ced-4(n1162)* were obtained from the CGC.

Genetic mapping, cloning, and sequencing

The *ep347* deletion allele of *cep-1* was identified by standard PCR-based methods (Jansen et al., 1997). *ep347* removes exons 9–13 and blocks DNA-damage-induced apoptosis to a similar extent as mutations in *hus-1* and *rad-5* (Supplemental Figure S6). The *cep-1 (ep347)* allele has this sequence across the deletion breakpoints: ACATTGATAATGTATCCAGGCGCAG/CATCCAGGAAGCGATGAAACTGCCA.

Mutagenesis and characterization were according to Epstein and Shakes (1995). The recessive increased-*g*erm*l*ine *a*poptosis (Gla) phenotype of the *ep402* mutant cosegregated with a recessive *m*aternal *e*ffect *l*ethal (Mel) phenotype. The Mel phenotype was mapped relative to single nucleotide polymorphisms between CB4586 and N2 (var. Bristol) (detected as described by Swan et al., 2002) to a 113 Kb interval between the regions contained in cosmids Y34B4A and C26B9. RNAi against the 20 predicted genes in this interval produced a Gla phenotype for only two: *Y34B4A.1* and *F32A6.3*. Transcript analysis showed that *Y34B4A.1* and *F32A6.3* represent a single gene. *ep402* is a nonsense mutation (UGG → UGA) at codon 523 in predicted exon 9 of *F32A6.3*.

Treatment of worms with RNAi reagents

RNAi reagents were generated by PCR amplification from a *C. elegans* genomic DNA template using *LA Taq* (Takara). Gene-specific priming sequences (Supplemental Table S5) were flanked by the T7 polymerase priming site. Amplicons typically spanned at least 1 kb and comprised exons. RNA was transcribed using the MEGAscript High Yield Transcription Kit (Ambion) and annealed at 68°C for 20 min. PCR product size

and quality of double-stranded RNA (dsRNA) were confirmed by gel electrophoresis. dsRNA was precipitated and resuspended in 20 mM KPO_4, 3 mM potassium citrate, 2% PEG 6000. For RNAi treatment, 1 μl of M9 buffer containing ~50 L3 worms was added to 3 μl of dsRNA (~5 mg/ml) and incubated for 24 hr in a sealed 96-well plate at 20°C, then plated on NGM plates seeded with OP50 bacteria for 24 hr before compound treatment and/or apoptosis assays.

Compound inhibition of RabGGT activity

For in vitro analysis, a filter binding assay was modified from Armstrong et al. (1995) and Shen and Seabra (1996). Reactions contained 50 mM HEPES (pH 7.4), 5 mM $MgCl_2$, 1 mM DTT, 1 mM NP-40, 2 μM human Rab3A (Panvera), 0.2 μM human REP-1 (Calbiochem), 2% DMSO, 10–50 nM rat RabGGT (Calbiochem), 5 μM unlabeled GPP (Sigma), and 0.5 μM labeled GGPP (Amersham Pharmacia Biotech; 15 Ci/mmol). After 30 min at 37°C, proteins were precipitated and collected onto GF/A filters (Whatman). Scintillation count data was analyzed with PRIZM (GraphPad Software, Inc.). For cellular assays, A549 cells were treated with BMS1 or BMS4 with 20 μM Z-VAD-FMK (Promega). After osmotic lysis, membranes were pelleted and the cytoplasmic extracts were blotted using antibodies sc-598 and sc-520 (Santa Cruz).

Design and validation of siRNA oligonucleotides

After validation (Supplemental Figures S2–S4), the siRNAs synthesized (Dharmacon Inc; Reynolds et al., 2004) were α-2 (GCACCUGGCTCACAAGGAU) and α-4 (CGACAGACGAGCAGCUAUU) (against *RabGGT-α*), β-3 (GAGAAUGAGUGGCAUCUAU) and β-4 (UUACUUGGCUGGUGGCUUU) (against *RabGGT-β*), control (AAGGGACGAAGACGAACACUUC; Firefly luciferase) and D-004098-02 (against *XIAP*).

Apoptosis assays in mammalian cells

Triplicate samples of cells in RPMI/10% FBS were treated with compound at the stated doses, or transfected using 20–25 nM siRNA and 2 μg/ml LipofectAMINE 2000 reagent (Invitrogen) in a final volume of 100 μl. Where indicated, Z-VAD-FMK (20 μM; Promega) was included. A549 cells (10,000/well) were processed with the Apo-one Caspase-3/7 assay (Promega). A2780 cells (2,000/well) were processed using the Cell Death Detection ELISA Plus assay (Roche). PC3 cells (2000/well) were fixed with 2% formaldehyde and stained with Hoechst and antibodies for activated caspase 3 and cytochrome C (Promega). Arrayscan 4.0 and the Target Activation application (Cellomics Inc.) were used to analyze 2,000–25,000 cells per treatment. Thresholds were set 1 standard deviation from median of negative control.

qRT-PCR analysis of mRNA expression

Total RNA was isolated from tissue samples using RNeasy (Qiagen), or was obtained from outside sources (Impath Predictive Oncology, Franklin, MA; Ardais Corporation, Lexington, MA; Genomics Collaborative, Cambridge, MA; University of California, Davis, CA). For breast, colon, lung, prostate, and ovary tumors, 21–33 unique tumor samples were analyzed; for other tissue types, 11–24 tumor samples were utilized. Preparation of cDNA and qPCR using SYBR-green was performed with a 7900HT instrument (Applied Biosystems). Data was analyzed using the application SDS (Applied Biosystems). Expression levels were normalized to 18S ribosomal RNA. Relative quantity units were calculated from a 5-point standard curve obtained using Universal Human Reference RNA (Stratagene).

Supplemental Data

Supplemental Data are available online at http://www.cancercell.org/cgi/content/full/7/4/325/DC1/.

Acknowledgments

We thank the CGC for worm strains. We thank B. Burley, D. Curtis, L. Friedman, J. Kelleher, J. Kopczynski, N. Laing, M. Maxwell, M. Nicoll, S. Ogg, D. Ruddy, B. Rupnow, R. Ryseck, T. Stouch, K. Swan, and S. Wong for contributions and support. We thank J. Margolis, N. Siemers, and R. Choy for helpful comments. This research was funded by Bristol-Myers Squibb and Exelixis Incorporated.

Received: August 3, 2004
Revised: November 5, 2004
Accepted: March 23, 2005
Published: April 18, 2005

References

Armstrong, S.A., Brown, M.S., Goldstein, J.L., and Seabra, M.C. (1995). Preparation of recombinant Rab geranylgeranyltransferase and Rab escort proteins. Methods Enzymol. *257*, 30–41.

Ashar, H.R., James, L., Gray, K., Carr, D., Black, S., Armstrong, L., Bishop, W.R., and Kirschmeier, P. (2000). Farnesyl transferase inhibitors block the farnesylation of CENP-E and CENP-F and alter the association of CENP-E with the microtubules. J. Biol. Chem. *275*, 30451–30457.

Bell, I.M., Gallicchio, S.N., Abrams, M., Beese, L.S., Beshore, D.C., Bhimnathwala, H., Bogusky, M.J., Buser, C.A., Culberson, J.C., Davide, J., et al. (2002). 3-Aminopyrrolidinone farnesyltransferase inhibitors: Design of macrocyclic compounds with improved pharmacokinetics and excellent cell potency. J. Med. Chem. *45*, 2388–2409.

Bishop, A.L., and Hall, A. (2000). Rho GTPases and their effector proteins. Biochem. J. *348*, 241–255.

Britten, C.D., Rowinsky, E.K., Soignet, S., Patnaik, A., Yao, S.L., Deutsch, P., Lee, Y., Lobell, R.B., Mazina, K.E., McCreery, H., et al. (2001). A phase I and pharmacological study of the farnesyl protein transferase inhibitor L-778,123 in patients with solid malignancies. Clin. Cancer Res. *7*, 3894–3903.

Cheng, K.W., Lahad, J.P., Kuo, W.L., Lapuk, A., Yamada, K., Auersperg, N., Liu, J., Smith-McCune, K., Lu, K.H., Fishman, D., et al. (2004). The RAB25 small GTPase determines aggressiveness of ovarian and breast cancers. Nat. Med. *10*, 1251–1256.

Clarke, S. (1992). Protein isoprenylation and methylation at carboxyl-terminal cysteine residues. Annu. Rev. Biochem. *61*, 355–386.

Coxon, F.P., Helfrich, M.H., Larijani, B., Muzylak, M., Dunford, J.E., Marshall, D., McKinnon, A.D., Nesbitt, S.A., Horton, M.A., Seabra, M.C., et al. (2001). Identification of a novel phosphonocarboxylate inhibitor of Rab geranylgeranyl transferase that specifically prevents Rab prenylation in osteoclasts and macrophages. J. Biol. Chem. *276*, 48213–48222.

Curtin, M.L., Florjancic, A.S., Cohen, J., Gu, W.Z., Frost, D.J., Muchmore, S.W., and Sham, H.L. (2003). Novel and selective imidazole-containing biphenyl inhibitors of protein farnesyltransferase. Bioorg. Med. Chem. Lett. *13*, 1367–1371.

Deneka, M., Neeft, M., and van der Sluijs, P. (2003). Regulation of membrane transport by rab GTPases. Crit. Rev. Biochem. Mol. Biol. *38*, 121–142.

Derry, W.B., Putzke, A.P., and Rothman, J.H. (2001). *Caenorhabditis elegans* p53: Role in apoptosis, meiosis, and stress resistance. Science *294*, 591–595.

Detter, J.C., Zhang, Q., Mules, E.H., Novak, E.K., Mishra, V.S., Li, W., McMurtrie, E.B., Tchernev, V.T., Wallace, M.R., Seabra, M.C., et al. (2000). Rab geranylgeranyl transferase alpha mutation in the gunmetal mouse reduces Rab prenylation and platelet synthesis. Proc. Natl. Acad. Sci. USA *97*, 4144–4149.

Du, W., Lebowitz, P.F., and Prendergast, G.C. (1999a). Cell growth inhibition by farnesyltransferase inhibitors is mediated by gain of geranylgeranylated RhoB. Mol. Cell. Biol. *19*, 1831–1840.

Du, W., Liu, A., and Prendergast, G.C. (1999b). Activation of the PI3′K-AKT pathway masks the proapoptotic effects of farnesyltransferase inhibitors. Cancer Res. *59*, 4208–4212.

DuHadaway, J.B., Du, W., Donover, S., Baker, J., Liu, A.X., Sharp, D.M., Muller, A.J., and Prendergast, G.C. (2003). Transformation-selective apoptotic program triggered by farnesyltransferase inhibitors requires Bin1. Oncogene *22*, 3578–3588.

Edinger, A.L., Cinalli, R.M., and Thompson, C.B. (2003). Rab7 prevents growth factor-independent survival by inhibiting cell-autonomous nutrient transporter expression. Dev. Cell *5*, 571–582.

End, D.W., Smets, G., Todd, A.V., Applegate, T.L., Fuery, C.J., Angibaud, P., Venet, M., Sanz, G., Poignet, H., Skrzat, S., et al. (2001). Characterization of the antitumor effects of the selective farnesyl protein transferase inhibitor R115777 in vivo and in vitro. Cancer Res. *61*, 131–137.

Epstein, H., and Shakes, D., eds. (1995). *Caenorhabditis elegans*: Modern Biological Analysis of an Organism (San Diego: Academic Press).

Gartner, A., Milstein, S., Ahmed, S., Hodgkin, J., and Hengartner, M.O. (2000). A conserved checkpoint pathway mediates DNA damage–induced apoptosis and cell cycle arrest in C. elegans. Mol. Cell *5*, 435–443.

Gumienny, T.L., Lambie, E., Hartwieg, E., Horvitz, H.R., and Hengartner, M.O. (1999). Genetic control of programmed cell death in the *Caenorhabditis elegans* hermaphrodite germline. Development *126*, 1011–1022.

Head, J.E., and Johnston, S.R. (2003). Protein farnesyltransferase inhibitors. Expert Opin. Emerg. Drugs *8*, 163–178.

Hengartner, M.O. (2001). Apoptosis: Corralling the corpses. Cell *104*, 325–328.

Hunt, J.T., Ding, C.Z., Batorsky, R., Bednarz, M., Bhide, R., Cho, Y., Chong, S., Chao, S., Gullo-Brown, J., Guo, P., et al. (2000). Discovery of (R)-7-cyano-2,3,4, 5-tetrahydro-1-(1H-imidazol-4-ylmethyl)-3- (phenylmethyl)-4-(2-thienylsulfonyl)-1H–1,4-benzodiazepine (BMS-214662), a farnesyltransferase inhibitor with potent preclinical antitumor activity. J. Med. Chem. *43*, 3587–3595.

Jansen, G., Hazendonk, E., Thijssen, K.L., and Plasterk, R.H. (1997). Reverse genetics by chemical mutagenesis in *Caenorhabditis elegans*. Nat. Genet. *17*, 119–121.

Jiang, K., Coppola, D., Crespo, N.C., Nicosia, S.V., Hamilton, A.D., Sebti, S.M., and Cheng, J.Q. (2000). The phosphoinositide 3-OH kinase/AKT2 pathway as a critical target for farnesyltransferase inhibitor-induced apoptosis. Mol. Cell. Biol. *20*, 139–148.

Jin, F., Wienecke, R., Xiao, G.H., Maize, J.C., Jr., DeClue, J.E., and Yeung, R.S. (1996). Suppression of tumorigenicity by the wild-type tuberous sclerosis 2 (Tsc2) gene and its C-terminal region. Proc. Natl. Acad. Sci. USA *93*, 9154–9159.

Levicar, N., Dewey, R.A., Daley, E., Bates, T.E., Davies, D., Kos, J., Pilkington, G.J., and Lah, T.T. (2003). Selective suppression of cathepsin L by antisense cDNA impairs human brain tumor cell invasion in vitro and promotes apoptosis. Cancer Gene Ther. *10*, 141–151.

Lewis, J.A., Wu, C.H., Levine, J.H., and Berg, H. (1980). Levamisole-resistant mutants of the nematode *Caenorhabditis elegans* appear to lack pharmacological acetylcholine receptors. Neuroscience *5*, 967–989.

Long, S.B., Casey, P.J., and Beese, L.S. (2002). Reaction path of protein farnesyltransferase at atomic resolution. Nature *419*, 645–650.

Makin, G. (2002). Targeting apoptosis in cancer chemotherapy. Expert Opin. Ther. Targets *6*, 73–84.

Manne, V., Lee, F.Y., Bol, D.K., Gullo-Brown, J., Fairchild, C.R., Lombardo, L.J., Smykla, R.A., Vite, G.D., Wen, M.L., Yu, C., et al. (2004). Apoptotic and cytostatic farnesyltransferase inhibitors have distinct pharmacology and efficacy profiles in tumor models. Cancer Res. *64*, 3974–3980.

Miaczynska, M., Christoforidis, S., Giner, A., Shevchenko, A., Uttenweiler-Joseph, S., Habermann, B., Wilm, M., Parton, R.G., and Zerial, M. (2004). APPL proteins link Rab5 to nuclear signal transduction via an endosomal compartment. Cell *116*, 445–456.

Momose, S., Kobayashi, T., Mitani, H., Hirabayashi, M., Ito, K., Ueda, M., Nabeshima, Y., and Hino, O. (2002). Identification of the coding sequences responsible for Tsc2-mediated tumor suppression using a transgenic rat system. Hum. Mol. Genet. *11*, 2997–3006.

Nakamura, N., Hirata, A., Ohsumi, Y., and Wada, Y. (1997). Vam2/Vps41p and Vam6/Vps39p are components of a protein complex on the vacuolar membranes and involved in the vacuolar assembly in the yeast *Saccharomyces cerevisiae*. J. Biol. Chem. *272*, 11344–11349.

Pei, L., Peng, Y., Yang, Y., Ling, X.B., Van Eyndhoven, W.G., Nguyen, K.C., Rubin, M., Hoey, T., Powers, S., and Li, J. (2002). PRC17, a novel oncogene encoding a Rab GTPase-activating protein, is amplified in prostate cancer. Cancer Res. *62*, 5420–5424.

Pfeffer, S.R., Dirac-Svejstrup, A.B., and Soldati, T. (1995). Rab GDP dissociation inhibitor: Putting rab GTPases in the right place. J. Biol. Chem. *270*, 17057–17059.

Prendergast, G.C., and Rane, N. (2001). Farnesyltransferase inhibitors: Mechanism and applications. Expert Opin. Investig. Drugs *10*, 2105–2116.

Reid, T.S., and Beese, L.S. (2004). Crystal structures of the anticancer clinical candidates R115777 (Tipifarnib) and BMS-214662 complexed with protein farnesyltransferase suggest a mechanism of FTI selectivity. Biochemistry *43*, 6877–6884.

Ren, Z., Elson, C.E., and Gould, M.N. (1997). Inhibition of type I and type II geranylgeranyl-protein transferases by the monoterpene perillyl alcohol in NIH3T3 cells. Biochem. Pharmacol. *54*, 113–120.

Reynolds, A., Leake, D., Boese, Q., Scaringe, S., Marshall, W.S., and Khvorova, A. (2004). Rational siRNA design for RNA interference. Nat. Biotechnol. *22*, 326–330.

Rose, W.C., Lee, F.Y., Fairchild, C.R., Lynch, M., Monticello, T., Kramer, R.A., and Manne, V. (2001). Preclinical antitumor activity of BMS-214662, a highly apoptotic and novel farnesyltransferase inhibitor. Cancer Res. *61*, 7507–7517.

Salgame, P., Varadhachary, A.S., Primiano, L.L., Fincke, J.E., Muller, S., and Monestier, M. (1997). An ELISA for detection of apoptosis. Nucleic Acids Res. *25*, 680–681.

Schumacher, B., Hofmann, K., Boulton, S., and Gartner, A. (2001). The *C. elegans* homolog of the p53 tumor suppressor is required for DNA damage-induced apoptosis. Curr. Biol. *11*, 1722–1727.

Seabra, M. (2000). Biochemistry of Rab geranylgeranyl transferase. In The Enzymes, F. Tamanoi and D. Sigman, eds. (New York: Academic Press), pp. 131–154.

Seabra, M.C., Mules, E.H., and Hume, A.N. (2002). Rab GTPases, intracellular traffic and disease. Trends Mol. Med. *8*, 23–30.

Seals, D.F., Eitzen, G., Margolis, N., Wickner, W.T., and Price, A. (2000). A Ypt/Rab effector complex containing the Sec1 homolog Vps33p is required for homotypic vacuole fusion. Proc. Natl. Acad. Sci. USA *97*, 9402–9407.

Shen, F., and Seabra, M.C. (1996). Mechanism of digeranylgeranylation of Rab proteins. Formation of a complex between monogeranylgeranyl-Rab and Rab escort protein. J. Biol. Chem. *271*, 3692–3698.

Slee, E.A., O'Connor, D.J., and Lu, X. (2004). To die or not to die: How does p53 decide? Oncogene *23*, 2809–2818.

Stergiou, L., and Hengartner, M.O. (2004). Death and more: DNA damage response pathways in the nematode *C. elegans*. Cell Death Differ. *11*, 21–28.

Strausberg, R.L., and Schreiber, S.L. (2003). From knowing to controlling: A path from genomics to drugs using small molecule probes. Science *300*, 294–295.

Strickland, C.L., Windsor, W.T., Syto, R., Wang, L., Bond, R., Wu, Z., Schwartz, J., Le, H.V., Beese, L.S., and Weber, P.C. (1998). Crystal structure of farnesyl protein transferase complexed with a CaaX peptide and farnesyl diphosphate analogue. Biochemistry *37*, 16601–16611.

Swan, K.A., Curtis, D.E., McKusick, K.B., Voinov, A.V., Mapa, F.A., and Cancilla, M.R. (2002). High-throughput gene mapping in *Caenorhabditis elegans*. Genome Res. *12*, 1100–1105.

Tee, A.R., Manning, B.D., Roux, P.P., Cantley, L.C., and Blenis, J. (2003). Tuberous sclerosis complex gene products, Tuberin and Hamartin, control mTOR signaling by acting as a GTPase-activating protein complex toward Rheb. Curr. Biol. *13*, 1259–1268.

Thoma, N.H., Iakovenko, A., Owen, D., Scheidig, A.S., Waldmann, H., Goody, R.S., and Alexandrov, K. (2000). Phosphoisoprenoid binding specificity of geranylgeranyltransferase type II. Biochemistry *39*, 12043–12052.

Thoma, N.H., Iakovenko, A., Kalinin, A., Waldmann, H., Goody, R.S., and Alexandrov, K. (2001a). Allosteric regulation of substrate binding and product release in geranylgeranyltransferase type II. Biochemistry *40*, 268–274.

Thoma, N.H., Niculae, A., Goody, R.S., and Alexandrov, K. (2001b). Double prenylation by RabGGTase can proceed without dissociation of the monoprenylated intermediate. J. Biol. Chem. *276*, 48631–48636.

Venet, M., End, D., and Angibaud, P. (2003). Farnesyl protein transferase inhibitor ZARNESTRA R115777 - history of a discovery. Curr. Top. Med. Chem. *3*, 1095–1102.

Xiao, G.H., Shoarinejad, F., Jin, F., Golemis, E.A., and Yeung, R.S. (1997). The tuberous sclerosis 2 gene product, tuberin, functions as a Rab5 GTPase activating protein (GAP) in modulating endocytosis. J. Biol. Chem. *272*, 6097–6100.

Zhang, H., Seabra, M.C., and Deisenhofer, J. (2000). Crystal structure of Rab geranylgeranyltransferase at 2.0 A resolution. Struct. Fold. Des. *8*, 241–251.